THE PENNSYLVANIA STATE UNIVERSITY
SCHREYER HONORS COLLEGE

DEPARTMENT OF GEOSCIENCES

PLANKTONIC FORAMINIFERA SHELL RESPONSE TO THE PALEOCENE-EOCENE THERMAL MAXIMUM: EVIDENCE FOR *ACARININA SOLDADOENSIS* SHELL THINNING

TIMOTHY LOGAN LINDEMANN
Spring 2013

A thesis
submitted in partial fulfillment
of the requirements
for a baccalaureate degree
in Science
with honors in Geobiology

Reviewed and approved* by the following:

Timothy Bralower
Professor of Geosciences
Thesis Supervisor and Honors Adviser

Lee Kump
Department Head Geosciences
Faculty Reader

* Signatures are on file in the Schreyer Honors College.

ABSTRACT

High-precision analysis of planktonic foraminiferal shell weights reveals an abrupt decrease in mass at the onset of the Paleocene-Eocene thermal maximum (PETM) at Site 690 in the Weddell Sea. The decline observed in the dominant species *Acarinina soldadoensis* occurs at the onset of the carbon isotope excursion (CIE) interval. Comparison of the mass and inferred volume suggests a thinning of *A. soldadoensis* shell walls. The event does not correlate with the significant decrease in calcium carbonate, likely a result of chemical erosion, suggesting that the mass reduction is a primary feature. We speculate that the mass decrease represents a thinning of *A. soldadoensis* shell walls in response to lower carbonate saturation at the onset of the PETM.

TABLE OF CONTENTS

LIST OF FIGURES

ACKNOWLEDGEMENTS

I would like to thank my honors advisor and thesis supervisor, Dr. Timothy Bralower, for his guidance and contributions to this thesis. His knowledge and support have been true assets throughout my research and college career. I also thank Dr. Lee Kump for his guidance and contributions to this thesis. I would like to thank Dr. Clay Kelly, from The University of Wisconsin – Madison, for training me in taxonomy and cleaning, picking, and sending me the foraminifera that were analyzed in this experiment. Without his assistance, this thesis would not have been possible. I acknowledge receipt of samples from the Integrated Ocean Drilling Program. I would like to express my gratitude to the members of the Penn State University faculty who motivated me to achieve success. Finally, I thank my friends and family for their constant encouragement and support as I pursue my goals.

Introduction

The release of massive amounts of carbon dioxide as a result of anthropogenic activities, "the great geophysical experiment" (Revelle and Seuss, 1957) has caused drastic change to Earth's environment. Global warming, melting of the ice caps, and sea level rise are all attributable to massive CO_2 emissions. About one third of the CO_2 added is dissolved in the ocean, which has caused a decrease in ocean pH and calcite and aragonite saturation leading to "ocean acidification" (Caldeira and Wickett, 2003). As fossil fuels continue to be burned, ocean pH and calcite/aragonite saturation will further decline; ultimately to such a point that calcification will prove challenging for many marine species (e.g., Donay et al., 2009; Hauri et al., 2009; Kleypas and Yates, 2009). Methods of determining the future implications of such drastic changes are becoming increasingly important.

Unfortunately, no computer model or laboratory experiment exists that can include all of the variables necessary to accurately predict how an enormously complex system, like the Earth, will behave in the future (e.g., Caldeira and Wickett, 2003). Thus, it is difficult to constrain the consequences of ocean acidification for the atmosphere and ocean surface waters. While similar emission events have occurred in Earth's history, the current rate of carbon dioxide emission has no precedent (Kump et al., 2009). However, the geologic record – which is not without its own limitations – may hold insights into how the ocean might respond to the continued rapid addition of CO_2.

The Paleocene-Eocene thermal maximum (PETM) is a geologically short-lived (~200,000 years) interval of accelerated warming that took place around 55.8 million years ago. With an onset of about 10-20 kyr, the rate of climate warming is slightly slower than the present (Kennett and Stott, 1991; Cui et al., 2011; Urban et al., in review). The event was characterized

by a significant warming of sea surface and deep ocean waters (~5-9°C) and a shoaling of the calcite compensation depth (CCD) to less than 2000 m (Kennett and Stott, 1991; Zachos et al., 2001, 2003, 2005). A precipitous decrease (~4-4.5%) in the carbon isotopic compositions of marine and terrestrial materials accompanies the warming, indicating a major disturbance in the global carbon cycle (Koch et al., 1992; Kennett and Stott, 1991; Bralower et al., 1995; Zachos et al., 2001). The PETM is associated with a mass extinction of benthic foraminifera (Thomas, 1990, 1998) and dramatic changes in calcareous plankton (Kelly et al., 1996, 1998; Bralower, 2002). Studies of PETM calcareous plankton assemblage changes offer insight into how modern plankton will respond to ocean acidification, climate changes, and nutrient availability (Gibbs et al., 2006).

Planktonic foraminifera are marine organisms that use calcium carbonate ($CaCO_3$) to build chambered shells. While shell thickness responses to more modern, Pleistocene glacial cycles have been studied (e.g., Broecker and Clark, 2001), no data on PETM foraminifera thickness variation exists. Analysis of planktonic foraminiferal mass, size, and shell thickness at various core depths could yield insights into changes of calcite saturation throughout the event. Analysis of the PETM foraminiferal shell morphology could be used to predict how modern foraminifera will physiologically respond to the modern "great geophysical experiment."

The goal of this investigation is to analyze changes in shell mass, size, and thickness of *Acarinina soldadoensis* and *Acarinina subsphaerica* from Hole 690B in the Southern Ocean. Site 690 contains the most expanded deep sea record of the PETM (e.g., Thomas et al., 2002; Kelly et al., 2005).

Methods

The PETM interval was sampled in Hole 690B, Core 19H, Sections 1–3. Site 690 (65°09'S, 01°12'E) is located on Maud Rise in the Weddell Sea, South Atlantic sector of the Southern Ocean (Figure 1). Samples were washed through a 63 μm sieve with dionized water buffered to pH 9-10 and oven dried. The samples were then dry sieved through 180, 250, and 300 μm sieves to separate the 180-250, 250-300, and >300 μm size fractions. Foraminiferal specimens were picked on picking trays. Whenever possible, analyses were carried out on *Acarinina soldadoensis*; *Acarinina subsphaerica* was analyzed in samples from the top of the study section where *A. soldadoensis* was not present. *A. soldadoensis* was analyzed in the 250-300 μm size fraction that could be precisely weighed in the microbalance. However, *A. subsphaerica* was only present in the 180-250 μm size fraction; precision relative to mass was lower in this size range. Between 5 and 12 specimens of *A. soldadoensis* and 2 to 11 specimens of *A. subsphaerica* were analyzed.

A Mettler Toledo MX5 microbalance was used to weigh individual specimens. Weighing precision, determined through replicate analysis was ~0.82 μg (*A. soldadoensis*) and ~0.88 μg (*A. subsphaerica*). Images of the umbilical views of specimens were acquired using a Canon PowerShot G9 camera, mounted on a Zeiss Stemi 2000-C binocular light microscope (magnification up to 100X). Areal measurement of specimens were determined in *ImageJ* using a calibration scale bar of 1000 μm. Finally, foraminiferal volumes were estimated in order to accurately scale variation in mass and size. Accurate scaling is important for assessing shell thickness throughout the section. Volumes were estimated according to the following equations:

Shell area = $\pi(r)^2$

Shell volume = $3/4\pi(r)^3$

For comparison, foraminiferal areas were assumed to be near-perfect circles, used to estimate the volume of near-perfect spheres. In this manner, previously determined shell areas were used to calculate the shell radii (r) according to equation (a). Shell volumes were then calculated by substituting the shell radii into equation (b). Shell mass/area/volume averages and standard deviations were determined for each interval.

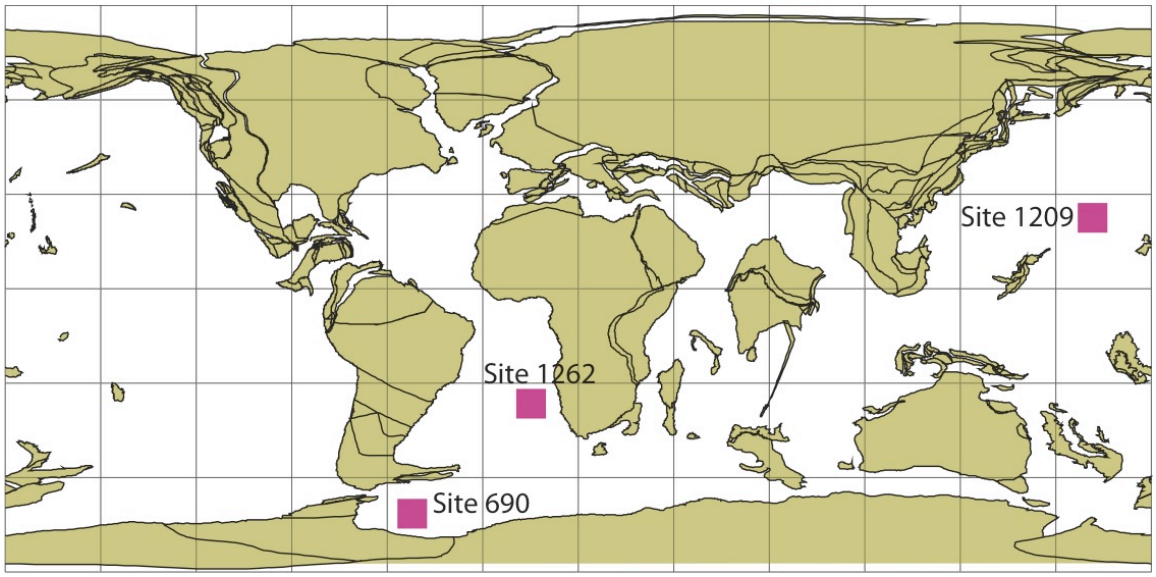

Figure 1: Global map of Site 690 in the Weddell Sea near Antarctica depicting the late Paleocene paleogeography (from Ocean Drilling Stratigraphic Network).

Results

Foraminiferal mass and area data are plotted versus depth, $\delta^{13}C$ and $CaCO_3$ (Figure 2); these data and inferred volume are plotted versus depth (Figure 3). Mean values for shell mass, area, and inferred volume are superimposed on the raw data to clarify trends. Plots of mass versus area and volume (Figure 4) are included to assess the scaling of mass and size. Plotted data are separated according to either *A. soldadoensis* or *A. subsphaerica*.

Throughout the study section, mass, area and inferred volume trends correlate with each other because of their direct correspondence to size. All three variables measured on *A. soldadoensis* show short-term variation in the basal part of the section (~169-171 m), as well as some longer-term trends. The key trend is a decrease in mean mass from ~18.0 μg to ~6.3 μg (~170.6-170.3 m) and a concomitant decrease in area from ~81,000 μm^2 to ~53,000 μm^2 (Figure 2). From ~170.3 to 169.3 mbsf, mass and area of *A. soldadoensis* appear to increase slightly. At the top of the section (~169-167 m), *A. subsphaerica* mass, area, and inferred volume data are fairly consistent; averaging ~2.5 μg, ~35,000 μm^2, ~3,000,000 μm^3 (Figure 3), respectively. The decrease in mass and area at ~170.6 mbsf is correlative with the base of the $\delta^{13}C$ excursion (Figure 2). The prominent decrease in $CaCO_3$ values at 170.8 mbsf precedes the decreases in mass and area (Figure 2). Overall, $\delta^{13}C$ is fairly consistent with mass and size trends, despite a recovery lag until ~169.5 mbsf (Figure 2). $CaCO_3$ values then increase at ~170.6 mbsf, preceding the recovery periods of mass and area (Figure 2). Inferred volume data (Figure 3) show the same trends as mass and area, averaging ~9,900,000 μm^3 at the peak and decreasing to ~5,100,000 μm^3 at ~170.4 mbsf before a slight recovery. According to Figure 4, mass shows a linear correlation with area and inferred volume. R-squared values are ~0.44 (*A. soldadoensis*) and ~0.10 (*A. subsphaerica*) for both area and inferred volume (Figure 4).

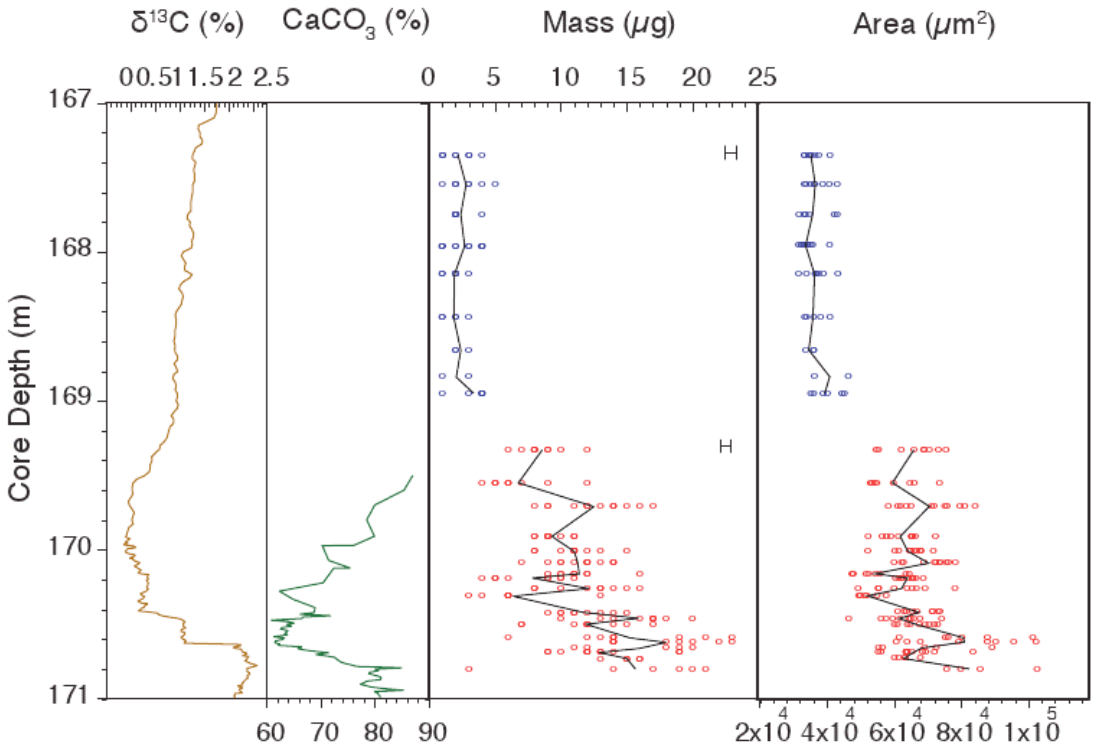

Figure 2: Stratigraphic change in $\delta^{13}C$, $CaCO_3$, and foraminiferal shell mass and area for the Hole 690B PETM section. Shell mass and area data sampled from *A. soldadoensis* (red) and *A. subsphaerica* (blue). Averages for data sets are superimposed over raw data. Mass precision was ~0.82 µg (*A. soldadoensis*) and ~0.88 µg (*A. subsphaerica*).

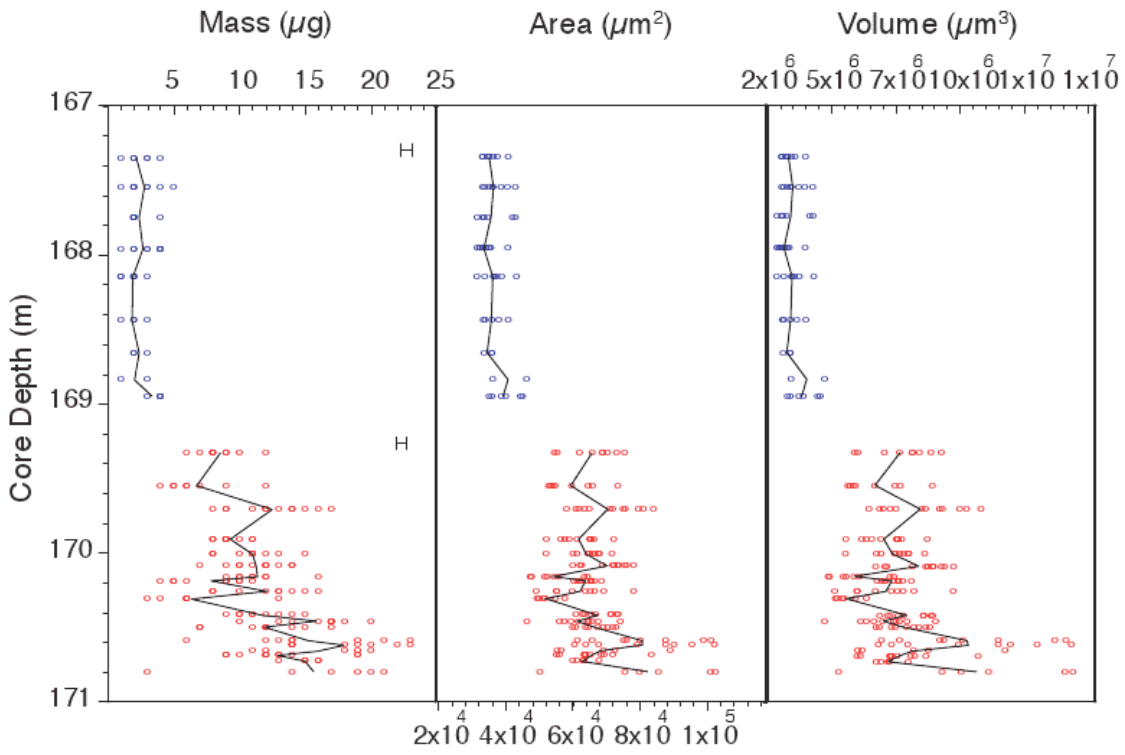

Figure 3: Stratigraphic change in foraminiferal shell mass, area, and inferred volume for Hole 690B PETM section. Shell data sampled from *A. soldadoensis* (red) and *A. subsphaerica* (blue). Averages for data sets are superimposed over raw data. Mass precision was ~0.82 µg (*A. soldadoensis*) and ~0.88 µg (*A. subsphaerica*).

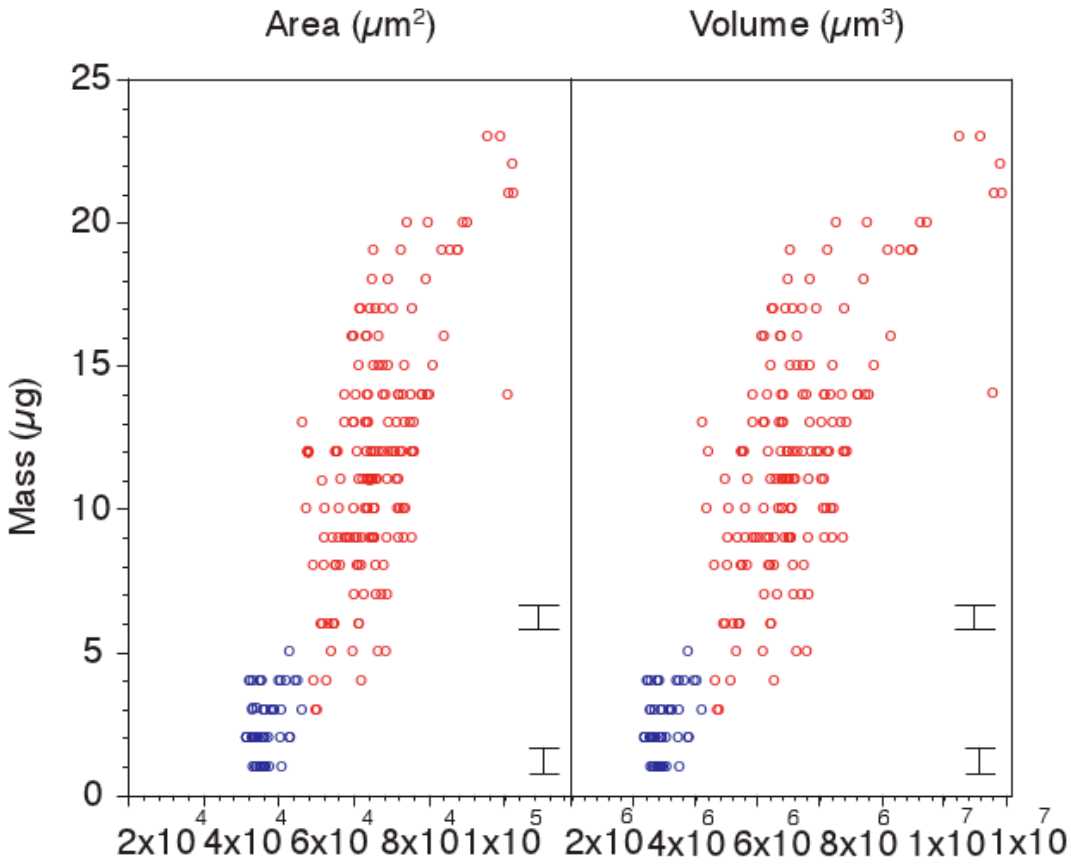

Figure 4: *A. soldadoensis* (red) and *A. subsphaerica* (blue) shell mass and inferred volume are plotted against mass. R-squared values for both area and volume are ~0.44 (*A. soldadoensis*) and ~0.10 (*A. subsphaerica*). Mass precision was ~0.82 µg (*A. soldadoensis*) and ~0.88 µg (*A. subsphaerica*).

Discussion

Scaling of Mass and Size

Determining accurate foraminiferal shell thickness is difficult. Foraminifera are microscopic organisms that can be too small to weigh on most balances and image in three dimensions with most microscopes. Accurate scaling of shell mass and size parameters is essential to determine if and how shell thickness changes throughout the study section.

The inferred volume estimate is an attempt to determine if the observed changes in mass are a direct function of changes in size or whether they represent primary changes in shell thickness (Figure 3). The inferred volume method provides a three dimensional estimation of shell dimensions but underestimates the actual volume because it does not account for the volume of chambers within the shell cavity. With this in mind, *A. soldadoensis* shell data (Figure 3) suggest a significant decrease in the peak mass and area during the early part of the PETM at Site 690. Average mass values shift from ~18.0 μg to ~6.3 μg; an overall decrease of ~65%. Average area values shift from ~81,000 μm^2 to ~53,000 μm^2; a decrease of ~35%. The average inferred volume values shift from ~9,900,000 μm^3 to ~5,100,000 μm^3; a decrease of ~48%. Thus, the average shell mass decreases ~30% more than area and ~17% more than inferred volume. Because mass decreases more relative to size, we argue that the average shell thickness significantly decreases. These results suggest that shell thickness was affected by dissolution rather than size reduction.

Potential Diagenetic Shell Alteration

Site 690 bulk carbon $\delta^{13}C$ isotope data (Figure 2; *Bains et al.,* 1999) provide an accurate framework for characterizing the chemical and biological evolution of the PETM. The carbon isotope excursion (CIE) can be divided into several stages: the pre-CIE interval, (171.42-170.63 m), which is associated with background conditions prior to the CIE; the CIE interval (170.63-169.60 m), which represents the core of the PETM, including the maximum chemical and biological perturbations; the CIE recovery interval (169.60-167.10 m) during which $\delta^{13}C$ ratios gradually return to background values and the environment recovers; and the post-CIE interval (167.10-165.94 m), which represents the earliest Eocene conditions.

The onset of the CIE appears to coincide with the observed key decrease in mass, area, and inferred volume. The abrupt decrease in $\delta^{13}C$ isotopes at this stage is attributed to rapid CO_2 addition to the atmosphere and ocean (e.g., Kennett and Stott, 1991; Dickens, 1995). CO_2 likely migrated from the surface ocean into the deep ocean reservoir where it caused a significant amount of carbonate dissolution (e.g., Zachos et al., 2005; Colosimo et al., 2006). The decrease in $CaCO_3$ values slightly precedes the $\delta^{13}C$, mass, and size decreases, likely as a result of chemical erosion, or burndown, in which previously deposited carbonate is dissolved when the saturation of deep waters declines (e.g., Dickens et al., 1997; Bralower et al., in revision). This dissolution could potentially remove mass and volume from foraminiferal shells.

Foraminiferal shell mass appears to peak during the pre-CIE interval, where $CaCO_3$ values are decreasing as a result of chemical erosion (Figure 2). It is possible that the dissolved $CaCO_3$ over-grew foraminiferal shells when saturation levels increased after the major pulse of dissolution. However, this process would not explain the sharp decrease in mass between 170.6 and 170.3 mbsf. We therefore interpret the shell mass decrease as a primary feature.

Change in Foraminiferal Morphology

Kelly (2002) described a profound increase in the percentage of "robust" *Acarinina* corresponding with the CIE_{bulk} onset (~170.63 m to 170.3) and the specimens analyzed in this interval were "robust." The observation that the "robust" *Acarinina* shells are in fact lighter than other taxa suggests that the exterior of this taxon masks thinner wall structure. The key decrease in *A. soldadoensis* shell mass, area, and inferred volume at the onset of the CIE interval (~170.6-170.3 m) suggests a unique lower saturation in ocean surface waters. Lower saturation is likely a result of rapid CO_2 dissolution (ocean acidification) during the PETM. This acute environmental change likely inhibited foraminifera shell formation, resulting in the observed size reduction and inferred thinning of shell walls.

Conclusions

During the Paleocene-Eocene thermal maximum (PETM) at Site 690 in the Weddell Sea, we observe a key decline in the dominant planktonic foraminifera species, *Acarinina soldadoensis*. The decline is characterized by a significant decrease in shell mass and size at the onset of the carbon isotope excursion (CIE) interval. Comparison of the mass and inferred volume suggests a thinning of *A. soldadoensis* shell walls, likely a result of CO_2 dissolution and ocean acidification. We argue that the mass reduction is a primary feature because the event does not correlate with the significant decrease in calcium carbonate, likely a result of chemical erosion. We postulate that observed thinning of shell walls was a response of calcification to lower carbonate saturation levels at the onset of the PETM.

References

Bains, S., R. M. Corfield, and R. D. Norris, 1999, Mechanisms of climate warming at the end of the Paleocene. *Science* 285, 724–727.

Bralower, T.J., 2002, Evidence for surface water oligotrophy during the late Paleocene thermal maximum: Nannofossil assemblage data from Ocean Drilling Program Site 690, Maud Rise, Weddell Sea. *Paleoceanography* 17,2, 13-1–13-3.

Bralower, T. J., J. C. Zachos, E. Thomas, M. Parrow, C. K. Paull, D. C. Kelly, I. Premoli Silva, W. V. Sliter, and K. C. Lohmann, 1995, Late Paleocene to Eocene paleoceanography of the equatorial Pacific Ocean: Stable isotopes recorded at ODP Site 865, Allison Guyot. *Paleoceanography* 10, 841–865.

Bralower, T.J., Kelly, D.C., Gibbs, S., Eccles, L., Lindemann, T.L., and Smith, G.J.. In revision. Impact of Carbonate Dissolution on the Sedimentary Record of the Paleocene-Eocene Thermal Maximum, EPSL.

Broecker, W.S. and Clark, E., 2001, Glacial-to-Holocene redistribution of carbonate ion in the deep sea. *Science* 294(5549), 2152-2155.

Caldeira, K., and M.E. Wickett, 2003, Anthropogenic carbon and ocean pH. *Nature* 425(6956), 365-365.

Colosimo, A. B., Bralower, T. J., and Zachos, J. C., 2006, Evidence for lysocline shoaling at the Paleocene/Eocene Thermal Maximum on Shatsky Rise, northwest Pacific. *In* Bralower, T.J., Premoli Silva, I., and Malone, M.J. (Eds.), *Proc. ODP, Sci. Results*, 198: College Station, TX (Ocean Drilling Program), 1–36, doi:10.2973/odp.proc.sr.198.112.

Cui, Y., Kump, L.R., Ridgwell, A.J., Charles, A.J., Junium, C.K., Diefendorf, A.F., Freeman, K.H., Urban, N.M., and Harding, I.C., 2011, Slow release of fossil carbon during the Palaeocene-Eocene Thermal Maximum. Nature Geoscience 4, 481-485, doi: 10.1038/NGEO1179.

Dickens, G.R., O'Neil, J.R., Rea, D.K., and Owen, R.M., 1995, Dissociation of oceanic methane hydrate as a cause of the carbon isotope excursion at the end of the Paleocene. *Paleoceanography* 10, 965–971.

Dickens, G. R., M. M. Castillo, and J. C. G. Walker, 1997, A blast of gas in the latest Paleocene: Simulating first-order effects of massive dissociation of oceanic methane hydrate. *Geology* 25, 259–262.

Doney, S.C., V. J. Fabry, R. A. Feely, and J. A. Kleypas, 2009, Ocean Acidification: The Other CO_2 Problem. Annual Review of Marine Science 1, 169-192, doi:10.1146/annurev.marine.010908.163834.

Gibbs, S.J., Bown, P.R., Sessa, J.A., Bralower, T.J., and Wilson, P.A., 2006a, Nannoplankton Extinction and Origination Across the Paleocene-Eocene Thermal Maximum. *Science* 314, 1770-1773.

Hauri, C., Gruber, N., Plattner, G.K., Alin, S., Feely, R.A., Hales, B., and Wheeler, P.A., 2009, Ocean Acidification in the California Current System. *Oceanography* 22(4):60–71, doi:10.5670/oceanog.2009.97.

Honisch, B., Ridgwell, A., Daniela N. Schmidt, Ellen Thomas Samantha J. Gibbs, Appy Sluijs, Richard Zeebe, Lee Kump, Rowan C. Martindale, Sarah E. Greene, Wolfgang Kiessling, Justin Ries, James C. Zachos, Dana L. Royer, Stephen BarkerThomas M. Marchitto Jr. Ryan Moyer, Carles Pelejero, Patrizia Ziveri, Gavin L. Foster, Branwen Williams, 2012,The Geological Record of Ocean Acidification. *Science* 335, 1058-1063.

Kelly, D.C., T.J. Bralower, J.C. Zachos, I. Premoli Silva, E. Thomas, 1996, Rapid diversification of planktonic foraminifera in the tropical Pacific (ODP Site 865) during the late Paleocene thermal maximum. *Geology* 24, 423-426.

Kelly, D. C., Bralower, T. J., and Zachos, J. C., 1998, Evolutionary consequences of the latest Paleocene thermal maximum for tropical planktonic foraminifera: *Palaeogeography*, *Palaeoclimatology*. *Palaeoecology* 141, 139-161.

Kelly, D. C., 2002. Response of Antarctic (ODP Site 690) planktonic foraminifera to the Paleocene-Eocene thermal maximum: faunal evidence for ocean/climate change. *Paleoceanography* 17, doi 10.1029/2002PA000761.

Kelly, D. C., Zachos, J. C., Bralower, T. J., and Schellenberg, S. A., 2005, Enhanced terrestrial weathering/runoff and surface ocean carbonate production during the recovery stages of the Paleocene-Eocene thermal maximum. *Paleoceanography* 20, PA4023, doi:10.1029/2005PA001163.

Kelly, D. C., Nielsen, T. M. J., and Schellenberg, S. A., 2012, Carbonate saturation dynamics during the Paleocene-Eocene thermal maximum: bathyal constraints from ODP Sites 689 and 690 in the Weddell Sea (South Atlantic). Marine Geology, doi: 10.1016/j.margeo.2012.02.003, in press.

Kennett, J.P. and L.D. Stott, 1991, Abrupt deep-sea warming, palaeoceanographic changes and benthic extinctions at the end of the Palaeocene, *Nature* 353, 225-229.

Kleypas, J.A. and Yates, K.K., 2009, Coral Reefs and Ocean Acidification. *Oceanography* 22(4):108–117, doi:10.5670/oceanog.2009.101.

Koch, P. L., J. C. Zachos, and P. D. Gingerich, 1992, Coupled isotopic change in marine and continental carbon reservoirs at the Palaeocene/Eocene boundary. *Nature* 358, 319–322.

Kump, L.R., Bralower, T.J., and Ridgwell A.R., 2009, Ocean acidification in deep time. *Oceanography* 22, 94-107.

McInerney, F.A., and Wing, S.L., 2011, The Paleocene-Eocene Thermal Maximum: A Perturbation of Carbon Cycle, Climate, and Biosphere with Implications for the Future. Ann. Rev. Earth Planet Sci. 39, 485.

Revelle, R., and H. Suess, 1957, Carbon dioxide exchange between atmosphere and ocean and the question of an increase of atmospheric CO2 during the past decades. *Tellus* 9, 18–27.

Ridgwell, A.T. and Schmidt, D.N., 2010. Past constraints on the vulnerability of marine calcifiers to massive carbon dioxide release. Nature Geoscience 3, 196-200, doi:10.1038/ngeo755.

Röhl, U., Westerhold, T., Bralower, T.J., and Zachos, J.C., 2007. On the duration of the Paleocene-Eocene thermal maximum. Geochemistry, Geophysics, Geosystems 8, (12), 3.1MB, www.agu.org/pubs/crossref/2007/2007GC001784.shtml, doi:10.1029/2007GC001784.

Thomas, E., 1990, Late Cretaceous – early Eocene mass extinctions in the deep sea, in *Global Catastrophes in Earth History: an Interdisciplinary Conference on Impacts, Volcanism, and Mass Mortality*, edited by V.L. Sharpton, and P. Ward. *GSA Spec. Publ. 247*, 481-496.

Thomas, E., 1998, Biogeography of the late Paleocene benthic foraminiferal extinction….. in *Late Paleocene-Eocene Climatic and Biotic Events in the Marine and Terrestrial Records*. M.-P. Aubry, S.G. Lucas, W.A. Berggren, eds, 214-243, Columbia Press, New York.

Thomas, D.J., J.C. Zachos, T.J. Bralower, E. Thomas, and S. Bohaty, 2002, Warming the fuel for the fire: Evidence for the thermal dissociation of methane hydrate during the Paleocene-Eocene thermal maximum. *Geology*.

Urban, N., Bralower, T.J., Haran, M., and Keller, K., A statistical interpretation of surface ocean temperature trends during the Paleocene-Eocene Thermal Maximum. *Paleoceanography*, in review.

Zachos, J. C., K. C. Lohmann, J. C. G. Walker, and S. W. Wise, 1993, Abrupt climate change and transient climates during the Paleogene: A marine perspective. *Geology* 101, 191–213.

Zachos, J. C., M. Pagani, L. Sloan, E. Thomas, and K. Billups, 2001, Trends, rhythms, and aberrations in global climate 65 Ma to present. *Science* 292, 686–693.

Zachos, J. C., M. W. Wara, S. Bohaty, M. L. Delaney, M. R. Petrizzo, A. Brill, T. J. Bralower, and I. Premoli-Silva, 2003, A transient rise in tropical sea surface temperature during the Paleocene-Eocene thermal maximum. *Science* 302, 1551–1554.

Zachos, J. C., U. Rohl, S. A. Schellenberg, A. Sluijs, D. A. Hodell, D. C. Kelly, E. Thomas, M. Nicolo, I. Raffi, L. J. Lourens, H. McCarren, and D. Kroon, 2005. Rapid acidification of the ocean during the Paleocene-Eocene Thermal Maximum. *Science* 308, 1611-1615.

ACADEMIC VITA

Timothy Logan Lindemann

1100 West Aaron Dr. Apt. D4
State College, PA 16803
tll5117@psu.edu

Education

B.S., Science; Biological Sciences and Health Professions Option, with honors in Geobiology, Spring 2013; The Pennsylvania State University, University Park, PA.

Honors and Awards

- Academic Excellence Scholarship, The Pennsylvania State University, 2009-13.

Association Memberships/Activities

- Alpha Epsilon Delta (AED) National Health Preprofessional Honor Society, Distinguished Membership, 2009-13.
- AED Public Health Fair, Spring 2010-2013.
- Camp Spifida (children's spina bifida camp), Counselor, Summer 2012.
- Intramural Flag Football Team, Fall 2009-10.
- Intramural Soccer Team, co-captain, Spring 2010-13.
- PSU/MSU Blood Donors Challenge and AED Blood Cup, Fall 2009-12.
- THON, 2009-13.

Research Experience

- Dr. Tim Bralower's Geobiology Lab, Undergraduate Research Assistant, 2010-13.
- Pediatric Nephrology Research at Geisinger Medical Center, Intern, Summer 2010.